

Complex Multinary Compounds from Molten Alkali Metal Polyselenophosphate Fluxes. Layers and Chains in $A_4Ti_2(P_2Se_9)_2(P_2Se_7)$ and $ATiPSe_5$ ($A = K, Rb$). Isolation of $[P_2Se_9]^{4-}$, a Flux Constituent Anion

Konstantinos Chondroudís and Mercuri G. Kanatzidis*

Department of Chemistry, Michigan State University, East Lansing, Michigan 48824

Received May 16, 1995

Recently, we suggested the use of polychalcophosphate fluxes for the synthesis of new ternary and quaternary thiophosphate and selenophosphate complexes.^{1–3} These fluxes are formed by simple *in situ* fusion of $A_2Q/P_2Q_5/Q$ and contain $[P_yQ_z]^{n-}$ ligands ($Q = S, Se$) which in the presence of metal ions coordinate to give, interesting new materials. We have shown that novel solid state structures can be constructed from $[P_2S_7]^{4-}$, $[PS_4]^{3-}$, and $[P_2Se_6]^{4-}$.^{1,2} Of course, quaternary compounds of this type have been prepared earlier by nonflux procedures at higher temperatures.³ The first compound reported from a $A_3P_3S_7$ flux reaction was $ABiP_2S_7$ ($A = K, Rb$).² The selenide containing fluxes gave rise to several unusual compounds such as $A_2MP_2Se_6$,^{3–5} KMP_2Se_6 ($M = Sb, Bi$),⁴ $Cs_8M_4(P_2Se_6)_5$ ($M = Sb, Bi$),³ $APbPSe_4$,⁶ $A_4Pb(PSe_4)_2$ ⁶ ($A = Rb, Cs$), and $K_4Eu(PSe_4)_2$.⁶ We have now investigated early transition metals such as Ti to explore whether this flux technique is applicable in this area of the periodic table, because it appears that no Ti/P/Q ternary or quaternary phases are known. Here we report the synthesis, structural characterization, and properties of the first selenophosphate quaternary titanium compounds, $Rb_4Ti_2(P_2Se_9)_2(P_2Se_7)$ and $KTiPSe_5$. One of the possible ligand anions present in these fluxes, namely $[P_2Se_9]^{4-}$, has been isolated as the Cs^+ salt and its structure is reported. All compounds feature novel structures containing the rare $[PSe_4]^{3-}$ as well as the polyselenido $[P_2Se_9]^{4-}$ and $[P_2Se_7]^{4-}$ ligands. The isostructural $K_4Ti_2(P_2Se_9)_2(P_2Se_7)$ and $RbTiPSe_5$ have also been prepared. The ability to vary the flux composition allows for control of basicity and consequently of the reaction pathway.^{4–6} One way is to vary the amount of A_2Se in the starting composition.⁶ In this case, however, access to each phase was achieved by varying the P_2Se_5 amount. Specifically, to obtain $A_4Ti_2(P_2Se_9)_2(P_2Se_7)$, a ratio of 1:3:2:10 of $Ti/P_2Se_5/A_2Se/Se$ was used. Changing the ratio to 1:2:2:10 gave $ATiPSe_5$.

$Rb_4Ti_2(P_2Se_9)_2(P_2Se_7)$ (**1**) has a layered structure; see Figure 1. The $[Ti_2(P_2Se_9)_2(P_2Se_7)]^{4-}$ layers are separated by six-coordinate $Rb(1)^+$ [$Rb(1)-Se$ mean = 3.6(1) Å] and eight-coordinate $Rb(2)^+$ ions [$Rb(2)-Se$ mean = 3.6(1) Å]. The layers form a perforated network made of $TiSe_6$ octahedra linked by $[P_2Se_7]^{4-}$ and $[P_2Se_9]^{4-}$ anions. The latter is a rare ligand and possesses a Se–Se–Se chain linking two phosphorus atoms. These layers contain very large 44-membered rings made of six titanium atoms, two $[P_2Se_7]^{4-}$ units, and four $[P_2Se_9]^{4-}$ units (ring dimensions: 26.61 Å along *a*-axis; 6.57 Å along *c*-axis).

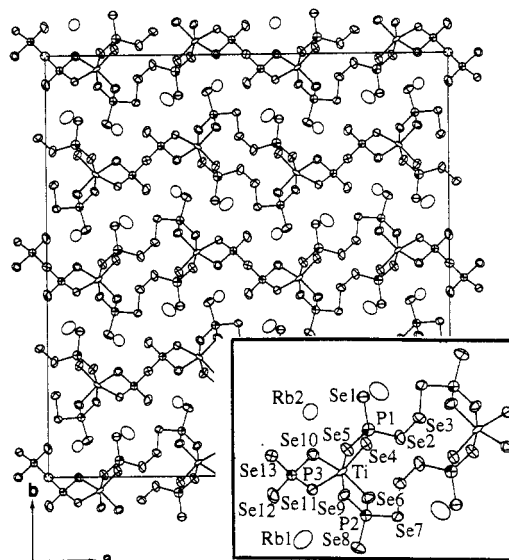


Figure 1. Structure of $Rb_4[Ti_2(P_2Se_9)_2(P_2Se_7)]$ viewed down the *c*-axis. Selected distances (Å): Ti–Se(4) 2.58(1), Ti–Se(5) 2.57(1), Ti–Se(6) 2.554(9), Ti–Se(9) 2.55(1), Ti–Se(10) 2.56(1), Ti–Se(11) 2.58(1), P(1)–Se(1) 2.14(1), P(1)–Se(2) 2.28(1), P(1)–Se(4) 2.20(1), P(1)–Se(5) 2.22(1), P(2)–Se(6) 2.21(1), P(2)–Se(7) 2.29(1), P(2)–Se(8) 2.13(1), P(2)–Se(9) 2.20(1), P(3)–Se(10) 2.20(1), P(3)–Se(11) 2.22(1), P(3)–Se(12) 2.13(1), P(3)–Se(13) 2.29(1), Se(2)–Se(3) 2.333(6). Selected angles (deg): Se(4)–Ti–Se(5) 83.6(3), Se(4)–Ti–Se(6) 102.1(3), Se(4)–Ti–Se(9) 92.1(3), Se(4)–Ti–Se(10) 85.4(3), Se(4)–Ti–Se(11) 162.1(4), Se(5)–Ti–Se(6) 88.6(3), Se(5)–Ti–Se(9) 169.8(4), Se(5)–Ti–Se(10) 106.1(3), Se(5)–Ti–Se(11) 85.0(3), Se(6)–Ti–Se(9) 83.2(3), Se(6)–Ti–Se(10) 164.3(4), Se(6)–Ti–Se(11) 91.3(3), Se(9)–Ti–Se(10) 82.7(3), Se(9)–Ti–Se(11) 101.2(3), Se(10)–Ti–Se(11) 84.5(2), Se(2)–Se(3)–Se(7) 103.7(2), Se(1)–P(1)–Se(2) 110.5(5), Se(1)–P(1)–Se(4) 114.9(6), Se(1)–P(1)–Se(5) 118.1(6), Se(2)–P(1)–Se(4) 108.7(6), Se(2)–P(1)–Se(5) 101.4(5), Se(4)–P(1)–Se(5) 102.1(5). Similar angles are observed around P(2) and P(3), min/max angles are 100.5(5)/117.4(6) and 102.7(5)/117.5(6), respectively.

The layers have a corrugated structure and they stagger by being offset along the *a*-axis by a $1/2$ translation. In a polyhedral description the titanium octahedra share edges with three phosphorus tetrahedra. Two of these tetrahedra belong to $[P_2Se_9]^{4-}$ units whereas the third one belongs to a $[P_2Se_7]^{4-}$ unit. The Ti–Se distances range from 2.554(9) to 2.58(1) Å. The P–Se distances range from 2.13(1) to 2.29(1) Å and compare well with those found in $APbPSe_4$.⁶

- (1) Sutorik, A.; Kanatzidis, M. G. *Prog. Inorg. Chem.*, in press.
- (2) (a) McCarthy, T. J.; Kanatzidis, M. G. *Chem. Mater.* **1993**, *5*, 1061. (b) McCarthy, T. J.; Hogan, T.; Kannewurf, C. R.; Kanatzidis, M. G. *Chem. Mater.* **1994**, *6*, 1072.
- (3) For examples see: (a) P. Toffoli, P. Khodadad, N. Rodier, *Acta Crystallogr.* **1977**, *B33*, 1492. (b) M. Z. Jandali, G. Eulenberger, H. Hahn, *Z. Anorg. Allg. Chem.* **1978**, *445*, 184. (c) Durand, E.; Evain, M.; Brec, R. *J. Solid State Chem.* **1992**, *102*, 146. (d) Toffoli, P.; Michelet, A.; Khodadad, P.; Rodier, N. *Acta Crystallogr.* **1982**, *B38*, 706. (e) D'ordyay, V. S.; Galagovets, I. V.; Peresh, E. Yu.; Voroshilov, Yu. V.; Gerasimenko, V. S.; Slivka, V. Yu. *Russ. J. Inorg. Chem. (Engl. Transl.)* **1979**, *24*, 1603.
- (4) McCarthy, T. J.; Kanatzidis, M. G. *J. Chem. Soc., Chem. Commun.* **1994**, 1089.
- (5) McCarthy, T. J.; Kanatzidis, M. G. *Inorg. Chem.* **1995**, *34*, 1257.
- (6) Chondroudís, K.; Kanatzidis, M. G. Submitted for publication.

- (7) (a) $A_4Ti_2(P_2Se_9)_2(P_2Se_7)$ ($A = K, Rb$) were synthesized from a mixture of Ti (0.3 mmol), P_2Se_5 (0.9 mmol), A_2Se (0.60), and Se (3 mmol) that was sealed under vacuum in a Pyrex tube and heated to 490 °C for 4 d followed by cooling to 150 °C at 4 °C h^{-1} . The excess $A_3P_3Se_7$ flux was removed with DMF to reveal black needles (88% yield based on Ti). The crystals are air- and water-stable. (b) Crystal data at –100 °C: $a = 35.55(1)$ Å, $b = 37.315(8)$ Å, $c = 6.574(7)$ Å, $V = 8722(10)$ Å³, $Z = 4$, $D_c = 3.956$ g cm^{-3} , space group $Fdd2$ (No. 43), $\mu(Mo K\alpha) = 255.74$ cm^{-1} , $2\theta_{max} = 50^\circ$, 2185 total data, 2185 unique data, 766 data with $F_o^2 > 3\sigma(F_o^2)$ variables. An empirical absorption correction based on ψ scans was applied to the data, followed by a (DIFABS)^{7c} correction to the isotropically refined data. All atoms except phosphorus were refined anisotropically. Final $R/R_w = 0.041/0.041$. (c) Walker, N.; Stuart, D. *Acta Crystallogr.* **1983**, *A39*, 158.

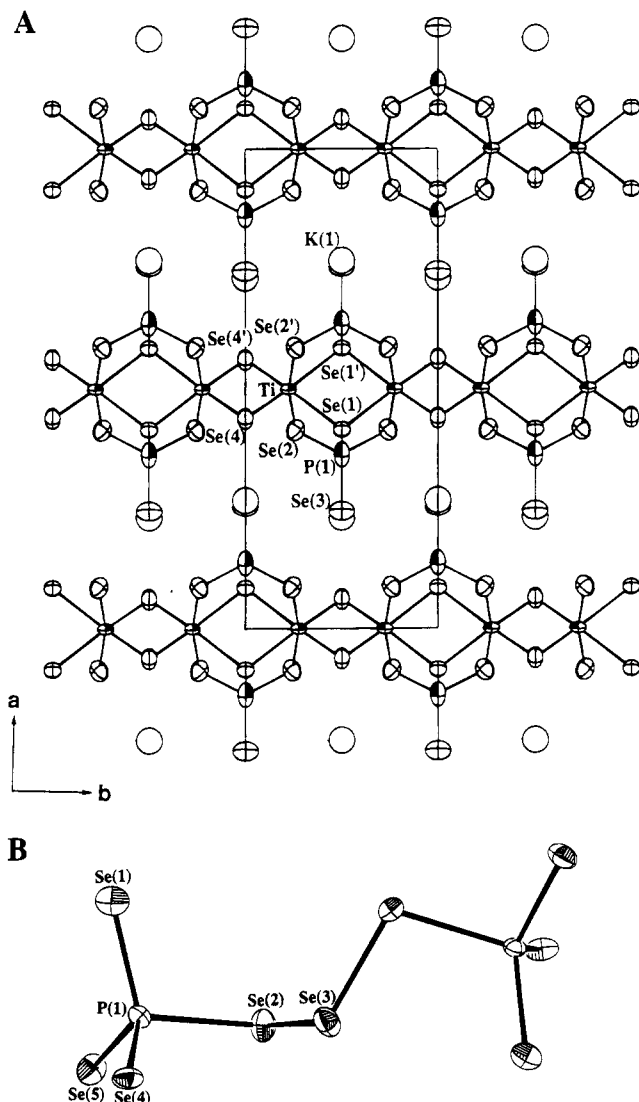


Figure 2. (A) KTiPSe_5 viewed down the c -axis. Selected distances (\AA): Ti–Se(1) 2.742(6), Ti–Se(2) 2.570(3), Ti–Se(4) 2.438(6), P(1)–Se(1) 2.25(1), P(1)–Se(2) 2.222(7) \AA , P(1)–Se(3) 2.13(1). Selected angles (deg): Se(1)–Ti–Se(1') 84.2(2), Se(1)–Ti–Se(2) 81.8(1), Se(1)–Ti–Se(2') 89.5(2), Se(1)–Ti–Se(4) 91.88(9), Se(1)–Ti–Se(4') 165.9(1), Se(2)–Ti–Se(2') 168.3(3), Se(2)–Ti–Se(4) 103.4(2), Se(2)–Ti–Se(4') 84.6(1), Se(4)–Ti–Se(4') 95.0(3), Se(1)–P(1)–Se(2) 102.2(4), Se(1)–P(1)–Se(3) 114.9(5), Se(2)–P(1)–Se(2') 105.9(4), Se(2)–P(1)–Se(3) 115.0(3), Ti–Se(1)–Ti 95.8(2), Ti–Se(1)–P(1) 85.2(2), Ti–Se(2)–P(1) 90.1(3), Ti–Se(4)–Ti 85.0(3). (B) Structure of the $[\text{P}_2\text{Se}_9]^{4-}$ anion.¹⁰

KTiPSe_5 (**II**) has the one-dimensional structure shown in Figure 2A. The chains consist of centrosymmetric $\text{Ti}_2(\text{PSe}_4)_2$ dimeric cores which are bridged by two $\mu_2\text{-Se}^{2-}$ ions. In these cores two $[\text{PSe}_4]^{3-}$ ligands bridge two octahedral titanium atoms employing three selenium atoms each. The fourth selenium remains nonbonding. The shortest Ti–Ti distance is between metals of adjacent dimers at 3.29(1) \AA . The Ti–Se distances range from 2.438(6) to 2.742(6) \AA and compare well with those found in **I**. The P–Se distances are similar to those of **I**. Finally, the chains are separated by eight coordinate K^+ ions [$\text{K}^+\text{-Se}$ mean 3.5(2) \AA].

- (8) (a) ATiPSe_5 compounds were synthesized from a mixture of Ti (0.2 mmol), P_2Se_5 (0.4 mmol), A_2Se (A = K, Rb) (0.40), and Se (2 mmol) under the same heating conditions as above, and they were isolated as above. The black, platelike crystals (79% yield based on Ti) are air- and water-stable. (b) Crystal data at -122°C : $a = 18.430(1)$ \AA , $b = 7.364(2)$ \AA , $c = 6.561(1)$ \AA , $\beta = 98.08(1)^\circ$, $V = 881.6(2)$ \AA^3 , $Z = 4$, $D_c = 3.863$ g cm^{-3} , space group C2/m (no. 12), $\mu(\text{Mo K}\alpha) = 219.69$ cm^{-1} , $2\theta_{\text{max}} = 50^\circ$, 869 total data, 840 unique data, 381 data with $F_o^2 > 3\sigma(F_o^2)$, 46 variables. Corrections were applied as above. Final $R/R_w = 0.059/0.081$.

$\text{Cs}_4\text{P}_2\text{Se}_9$ (**III**) was obtained in our attempt to isolate various $[\text{P}_x\text{Q}_z]^{n-}$ ligands thought to be present in polychalcophosphate fluxes. It consists of isolated $[\text{P}_2\text{Se}_9]^{4-}$ units which in turn are made of two PSe_4 subunits connected via a monoselenide (see Figure 2B). The presence of this polyselenido anion is not surprising, because these fluxes are always chalcogen-rich. The molecule is sitting on a 2-fold axis going through Se(3). There are two crystallographically independent Cs^+ ions, both having eight-coordinate environment [$\text{Cs}(1)\text{-Se}$ mean 3.80(9) \AA], [$\text{Cs}(2)\text{-Se}$ mean 3.74(7) \AA]. The potassium and rubidium analogs were also prepared and they are very air and moisture sensitive.

The optical spectra of the compounds show sharp optical gaps consistent with semiconductors. The $\text{Rb}_4\text{Ti}_2(\text{P}_2\text{Se}_9)_2(\text{P}_2\text{Se}_7)$ shows a band-gap, E_g , of 1.38 eV, while KTiPSe_5 and $\text{Cs}_4\text{P}_2\text{Se}_9$ show gaps of 1.06 and 1.78 eV respectively. The Raman spectra of **I** display shifts at ~ 504 , ~ 400 , ~ 266 , ~ 228 , ~ 186 , and ~ 156 cm^{-1} . Compound **III** displays shifts at ~ 475 , ~ 357 , ~ 265 , ~ 228 , and ~ 159 cm^{-1} . The shifts at ~ 266 and ~ 265 cm^{-1} in **I** and **III** are attributed to Se–Se stretching vibrations. Those at higher energies are due to P–Se vibrations. Compounds **I** and **II** melt incongruently at 403 and 525 $^\circ\text{C}$ respectively yielding TiSe_2 and $\text{A}_x\text{P}_y\text{Se}_x$. This highlights the value of the alkali polychalcophosphate flux which allows the synthesis of compounds at relatively low temperatures. Compound **III** melts congruently at 446 $^\circ\text{C}$.

The first selenophosphate titanium compounds have been prepared in molten polyselenophosphate $\text{A}_x[\text{P}_y\text{Se}_z]$ fluxes. The noncentrosymmetric $\text{A}_4\text{Ti}_2(\text{P}_2\text{Se}_9)_2(\text{P}_2\text{Se}_7)$ may be potentially interesting nonlinear optical materials. In the $\text{A}_x[\text{P}_y\text{Se}_z]$ system, unlike other fluxes (e.g. halide or metal fluxes), control of the flux composition permits to a certain degree control of the reaction outcome and thus can be exploited productively in synthetic solid-state chemistry. Selenophosphate systems containing different metal ions have also yielded novel solid-state structures.¹⁰ Furthermore, certain flux conditions can promote the crystallization of various $[\text{P}_y\text{Se}_z]^{n-}$ anions present in it. The isolation and identification of such anions will help understand better the nature of these fluxes and will provide useful insight into how the various multinary compounds form.

Note Added in Proof: During the preparation of this report, a paper appeared describing a possible S analog of **I**: Tremel, W.; Kleinke, H.; Derstroff, V.; Reisner, C. *J. Alloys Compd.* **1995**, 219, 73.

Acknowledgment. Financial support came from National Science Foundation Grant DMR-9202428.

Supporting Information Available: Tables of crystallographic details, fractional atomic coordinates of all atoms, anisotropic and isotropic thermal parameters of all atoms, interatomic distances and angles, and calculated and observed X-ray powder patterns for $\text{Rb}_4\text{-Ti}_2(\text{P}_2\text{Se}_9)_2(\text{P}_2\text{Se}_7)$ and KTiPSe_5 , and $\text{Cs}_4\text{P}_2\text{Se}_9$ (47 pages). Ordering information is given on any current masthead page.

IC950602X

- (9) (a) The red, air- and water-sensitive $\text{Cs}_4\text{P}_2\text{Se}_9$ was synthesized from a mixture of P_2Se_5 (0.45 mmol), Cs_2Se (1.20), and Se (3 mmol) with the same aforementioned heating conditions (80% yield based on P). (b) Unit cell at 25°C : $a = 10.163(1)$ \AA , $b = 10.582(2)$ \AA , $c = 19.655(2)$ \AA , $\beta = 94.02(1)^\circ$, $V = 2108.7(5)$ \AA^3 , $Z = 4$, $D_c = 4.108$ g cm^{-3} , space group C2/c (no. 15), $\mu(\text{Mo K}\alpha) = 223.28$ cm^{-1} , $2\theta_{\text{max}} = 50^\circ$, 2105 total data, 1979 unique data, 1420 data with $F_o^2 > 3\sigma(F_o^2)$, 70 variables. Corrections were applied as above. Final $R/R_w = 0.033/0.050$. Selected distances (\AA) are as follows: P(1)–Se(1) 2.157(4), P(1)–Se(2) 2.335(3), P(1)–Se(4) 2.166(4), P(1)–Se(5) 2.183(3), Se(2)–Se(3) 2.340(2). Selected angles (deg) are as follows: Se(1)–P(1)–Se(2) 108.6(1), Se(1)–P(1)–Se(4) 111.6(1), Se(1)–P(1)–Se(5) 115.5(1), Se(2)–P(1)–Se(4) 108.4(1), Se(2)–P(1)–Se(5) 95.5(1), Se(4)–P(1)–Se(5) 115.5(1), P(1)–Se(2)–Se(3) 101.32(9), Se(2)–Se(3)–Se(2) 111.7(1). Torsion angle around Se(2)–Se(3) bond: 108.8(1) $^\circ$.
- (10) Chondroudis, K.; Kanatzidis, M. G. To be submitted for publication.